

Dynamics of quantal heating in electron systems with discrete spectra

Scott Dietrich, William Mayer, and Sergey Vitkalov*

Physics Department, City College of the City University of New York, New York 10031, USA

A. A. Bykov

*A. V. Rzhanov Institute of Semiconductor Physics, Novosibirsk 630090, Russia**and Novosibirsk State University, Novosibirsk 630090, Russia*

(Received 9 October 2014; revised manuscript received 13 May 2015; published 27 May 2015)

The temporal evolution of quantal Joule heating of two-dimensional (2D) electrons in a GaAs quantum well placed in quantizing magnetic fields is studied using a difference-frequency method. The method is based on measurements of the electron conductivity oscillating at the beat frequency $f = f_1 - f_2$ between two microwaves applied to the 2D system at frequencies f_1 and f_2 . The method provides *direct* access to the dynamical characteristics of the heating and yields the inelastic-scattering time τ_{in} of 2D electrons. The obtained τ_{in} is strongly temperature dependent, varying from 0.13 ns at 5.5 K to 1 ns at 2.4 K in magnetic field $B = 0.333$ T. When the temperature T exceeds the Landau-level separation, the relaxation rate $1/\tau_{in}$ is proportional to T^2 , indicating electron-electron interaction as the dominant mechanism limiting the quantal heating. At lower temperatures, the rate tends to be proportional to T^3 , indicating considerable contribution from electron-phonon scattering.

DOI: [10.1103/PhysRevB.91.205439](https://doi.org/10.1103/PhysRevB.91.205439)

PACS number(s): 72.20.Ht, 73.43.Qt, 73.50.Jt, 73.63.Hs

Joule heating is a remarkable physical phenomenon which transforms electric energy into heat. Recently, it was shown that the quantum properties of matter significantly affect the heating [1,2], giving rise to a thermal stratification (quantization) of the electron distribution in energy space [3]. This effect, called quantal heating, does not exist in classical electron systems. The most essential property of quantal heating is the conservation of the total number of quantum states participating in the electron transport and, thus, the conservation of the overall broadening of the electron distribution [2,3]. In contrast to classical Joule heating, quantal heating leads to outstanding nonlinear transport properties of highly mobile two-dimensional (2D) electrons, driving them into exotic nonlinear states in which voltage (current) does not depend on current [4] (voltage) [5]. Quantal heating also provides significant contributions to nonlinear effects at high driving frequencies—an important topic in contemporary research [6].

Joule heating of 2D electrons in quantizing magnetic fields was observed in the pioneer work on 2D electron transport [7]. The heating decreased the amplitude of the Shubnikov–de Haas (SdH) oscillations of the conductivity, providing a way to measure the electron inelastic relaxation. Assuming that the distribution of overheated electrons is described by an electron temperature [8–21], the inelastic relaxation rate of 2D electrons in GaAs heterojunctions was found to be proportional to the temperature at a lattice temperature of few Kelvin [8,14,19]. This widely accepted result has been examined and a substantial inconsistency was found between inelastic relaxation times in zero and quantizing magnetic fields [19]. The SdH result was further challenged in recent investigations of Joule heating [2]. In these investigations, the temperature approximation of overheated electrons has been relaxed. Using a spectral diffusion equation [1], the

nonequilibrium electron distribution was evaluated numerically, revealing significant deviations from the Fermi-Dirac form. The temperature dependence of the inelastic relaxation rate obtained by this method was found to be considerably different from the expected: T^2 at $kT \gg \hbar\omega_c$ and T^3 at $kT \sim \hbar\omega_c$, where ω_c is cyclotron frequency [2]. These findings raise a concern regarding the validity of the inelastic relaxation time $\tau_{in}^{SdH}(T)$ obtained by the SdH method.

Here we present an experimental method which accesses the temporal evolution of electron transport under quantal Joule heating. The method provides the *direct* measurement of the inelastic relaxation time τ_{in} . At high temperatures, the time is found to be in good quantitative agreement with the inelastic time τ_{in}^{dc} obtained in dc experiments on quantal heating [2]. At low temperatures, a disagreement between these two times is observed. The temperature dependence of the inelastic time is found to be significantly different from the one obtained by the SdH method [8,14,19].

The dynamics of quantal heating was studied in a two-dimensional system of highly mobile electrons in Corbino geometry. The Corbino geometry provides effective suppression [5] of contributions from 1D edge channels [22,23] to the charge and heat transport [24–26]. The Corbino disk with inner radius $r_1 = 0.9$ mm and outer radius $r_2 = 1$ mm was fabricated from a selectively doped single GaAs quantum well sandwiched between AlAs/GaAs superlattice barriers. The width of the well was 13 nm. The structure was grown by molecular beam epitaxy on a (100) GaAs substrate. AuGe eutectic was used to provide electric contacts to the 2D electron gas. The 2D electron system with electron density $n = 8 \times 10^{15} \text{ m}^{-2}$ and mobility $\mu = 112 \text{ m}^2/\text{Vs}$ at $T = 4.8$ K was studied at different temperatures, from 2.4 to 6 K, in magnetic fields up to 1 T.

Figure 1 shows the experimental setup. Two microwave sources supply the radiation to the sample through a semirigid coax at two different frequencies (f_1 , f_2). The interference between these sources forms microwave radiation with amplitude modulation at the difference (beat) frequency

*Corresponding author: vitkalov@sci.ccny.cuny.edu

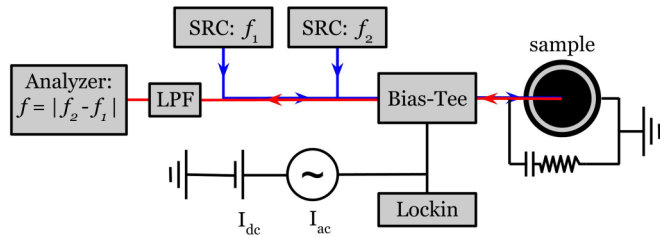


FIG. 1. (Color online) Experimental setup for the difference-frequency method. Two microwave sources (SRC) at frequencies f_1 and f_2 send radiation to the sample through broadband directional couplers. The microwave analyzer detects a signal at the difference frequency between the sources, $f = f_2 - f_1$. The incorporated RC circuit ($R = 50$ Ohm, $C = 47$ pF) provides broadband matching. A low-pass filter (LPF) blocks the high-frequency signals (f_1, f_2) from the analyzer. Bias current (I_{dc}) as well as low-frequency lock-in measurements (I_{ac}) are incorporated into the same universal measurement line through a bias tee.

$f = f_1 - f_2$. The modulated microwave induces oscillations of Joule heating and, thus, the sample resistance δR_f at the frequency f . Application of a dc current I_{dc} to the structure produces voltage oscillations $\delta V_f = \delta R_f I_{dc}$, which propagate back to a microwave analyzer through the same coax. The analyzer detects an amplitude of the voltage oscillations at frequency f (f signal). In addition, the setup contains a bias-tee providing measurements in the dc domain. These measurements are essential for a calibration of the microwave setup.

In experiments, the frequency $f_1 = 8$ GHz was fixed, while frequency f_2 was scanned from 5.5 to 7.999 GHz. To take into account variations of the microwave power P_2 delivered to the sample in the course of the frequency scan, a dc measurement of the resistance variation induced by the same applied microwave power P_2 is done. At a small applied power, the induced resistance variation is proportional to P_2 , thereby providing the power calibration. A similar calibration is done for the receiver channel at frequency f and is based on the reciprocal property of the microwave setup.

Figure 2 presents the magnetic field dependence of the resistance of the sample, R , with neither dc bias nor microwaves applied (thin solid line). At small magnetic fields ($B < 0.1$ T), the resistance shows the classical parabolic increase with the field [27]. At these fields, the Landau-level separation $\hbar\omega_c$ is much smaller than the level width $\Gamma = \hbar/\tau_q$, and both the quantization of the electron spectrum and quantal heating are exponentially small [1,2]. At higher magnetic field ($B > 0.1$ T), a deviation from the Drude behavior is observed. The deviation is related to quantum corrections to the magnetoconductivity [28] and yields the quantum scattering time [29] $\tau_q \approx 4.5$ ps at $T = 5.5$ K. The thick solid line presents the nonlinear response of the sample (f signal) measured at difference frequency $f = 1$ MHz. The response is very weak at small magnetic fields $B < 0.1$ T. Above 0.1 T, the modulation of the density of electron states (DOS) becomes observable and the nonlinear response grows strongly with the magnetic field. At higher magnetic fields ($\hbar\omega_c \gg \Gamma$), the exponential increase of the DOS modulation ceases and the nonlinear response decreases due to the shrinkage of

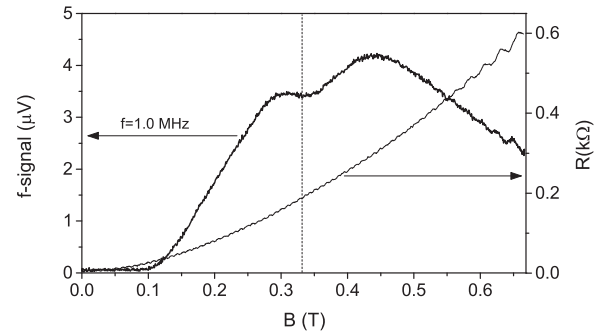


FIG. 2. Magnetic field dependences of the sample resistance R (right axis, thin line; no microwave and dc bias applied) and microwave analyzer signal (left axis, thick line) at the difference frequency $f = 1.0$ MHz with MW sources at powers $P_1(8$ GHz) = -22 dBm and $P_2(7.999$ GHz) = -19 dBm and with direct current $I_{dc} = 10$ μ A. The vertical dashed line indicates the magnetic field chosen for study of the frequency dependence of the nonlinear response: $B = 0.333$ T. $T = 4.8$ K.

electron orbits leading to reduction of the spatial and spectral electron diffusions [1,2]. At $T = 4.8$ K and $B > 0.5$ T, SdH oscillations are visible in both the resistance and the f signal. The frequency dependence of the f signal was studied at magnetic field $B = 0.333$ T, corresponding to a SdH maximum of the sample conductivity at low temperatures (not visible at $T = 4.8$ K).

Figure 3 presents the dependence of the f signal and differential resistance on the dc voltage V_{dc} at different frequencies f as labeled. At small dc biases, the f signal is proportional to V_{dc} , while variations of the differential resistance $\delta r \sim V_{dc}^2$. These data agree with the relation $j = \sigma_0 E + \alpha E^3$ between the current density j and the electric field E , which is expected for small fields. Here, σ_0 is the ohmic conductivity (linear response). In this perturbative regime, the nonlinear current density j_ω ($\sim f$ signal) at angular frequency $\omega = 2\pi f$ should be proportional to applied dc (E_0) and microwave (mw) (E_1, E_2) electric fields: $j_\omega = 3\alpha E_0 E_1 E_2$.

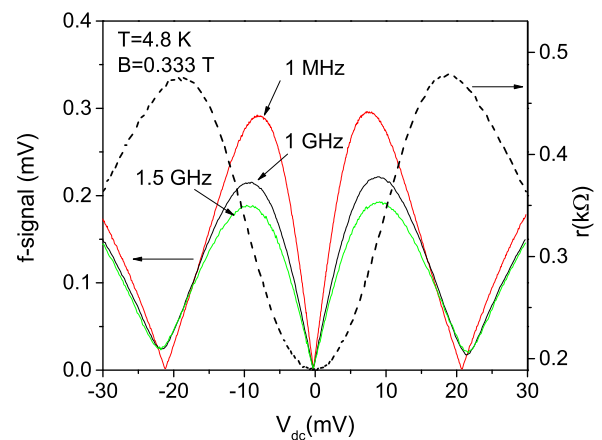


FIG. 3. (Color online) Dependence of the f signal on dc voltage, V_{dc} , applied to sample. The dependence is shown at different frequencies f as labeled. The dashed line presents the dc-bias dependence of differential resistance r obtained in the dc domain.

The observed microwave power dependence (not shown) of the f signal is in complete agreement with the expected behavior at small microwave power. The differential resistance demonstrates a maximum at $V_{dc} \approx 20$ mV. The maximum is related to a crossover between quantal heating and dc-bias-induced Landau-Zener transitions [30–32]. The f signal shows an additional interesting feature at higher dc biases, which were beyond the scope of the present work.

The frequency dependence of the nonlinear response can be understood from an analysis of the spectral diffusion equation for the electron distribution function $f(\epsilon)$ [1,2]:

$$-\frac{\partial f(\epsilon)}{\partial t} + E^2 \frac{\sigma_D}{v(\epsilon)} \partial_\epsilon [\tilde{v}^2(\epsilon) \partial_\epsilon f(\epsilon)] = \frac{f(\epsilon) - f_T(\epsilon)}{\tau_{in}}. \quad (1)$$

Here, σ_D is the Drude conductivity in a magnetic field B , $\tilde{v} = v/v_0$ is the ratio of the density of electron states (DOS) $v(\epsilon)$ to the DOS at zero magnetic field v_0 , and f_T represents the Fermi-Dirac distribution at a temperature T . Below we consider the case of a low difference frequency $\omega = \omega_1 - \omega_2 \ll \omega_1, \omega_2$ corresponding to the experiments ($\omega_i = 2\pi f_i$). At small electric field $E(t) = E_0 + E_1 \exp(i\omega_1 t) + E_2 \exp(i\omega_2 t)$, the distribution function can be written as $f(\epsilon) = f_T + \delta f_\omega$, where the oscillating distribution $\delta f_\omega \sim E_1 E_2 \exp[i(\omega_1 - \omega_2)t]$ is the leading contribution to the f signal. A substitution of this function into Eq. (1) yields the following solution for the electron distribution oscillating at difference frequency ω :

$$\delta f_\omega(\epsilon) = \frac{2E_1 E_2 \exp(i\omega t)}{i\omega + 1/\tau_{in}} \frac{\sigma_D}{v(\epsilon)} \partial_\epsilon [\tilde{v}^2(\epsilon) \partial_\epsilon f_T(\epsilon)]. \quad (2)$$

The oscillating electron distribution results in oscillations of the electric current density at frequency ω ,

$$j_\omega = E_0 \int \sigma_\epsilon [-\partial_\epsilon (\delta f_\omega)] d\epsilon = \frac{2E_0 E_1 E_2 \exp(i\omega t)}{i\omega + 1/\tau_{in}} \Sigma. \quad (3)$$

Here σ_ϵ is the conductivity at energy ϵ and $\Sigma = -\sigma_D \int \sigma_\epsilon \partial_\epsilon [\partial_\epsilon (\tilde{v}^2 \partial_\epsilon f_T)/v] d\epsilon$. Equation (3) indicates that at high difference frequency $\omega \gg 1/\tau_{in}$, the f signal is inversely proportional to frequency. In this regime, microwave radiation is “on” for a short time $\Delta t \sim 1/\omega$, which is not enough to considerably change the electron distribution.

Figure 4 presents the frequency dependence of the f signal at different temperatures as labeled. The observed f signal is nearly frequency independent at low frequencies and is inversely proportional to the frequency in the high-frequency limit. The solid lines represent the frequency dependence expected from Eq. (3), $j_\omega = A/|1 + i\omega\tau_{in}|$, with amplitude A and time τ_{in} as fitting parameters. The figure indicates good agreement between the data and the frequency dependence described by Eq. (3). The inset to the figure presents the temperature dependence of the inelastic-scattering time τ_{in} obtained from the fit. The high-temperature behavior of the inelastic time is consistent with the $1/T^2$ decrease, indicating the dominant contribution of electron-electron interactions to the inelastic electron relaxation. At low temperatures, a deviation from the $1/T^2$ behavior is found, indicating a suppression of the $e-e$ contribution. The suppression is expected at low temperatures, when $kT < \hbar\omega_c$. At this condition, the $e-e$ scattering is ineffective (see Fig. 7 in Ref. [2]), since the scattering conserves the total electron energy.

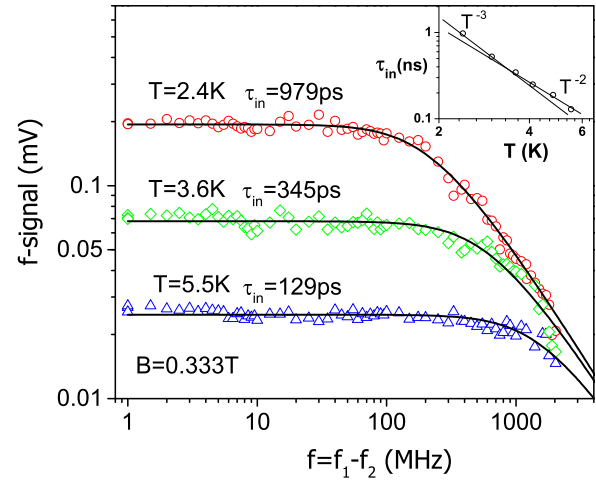


FIG. 4. (Color online) Frequency dependence of the f signal at different temperatures T as labeled. Solid lines present the dependence obtained from Eq. (3) using τ_{in} as a fitting parameter. Inset: The temperature dependence of the obtained inelastic-scattering time.

Below we compare the inelastic time τ_{in} with the time τ_{in}^{dc} obtained in the dc domain [2]. Figure 5(a) presents the dependence of the normalized conductivity [27] of the sample σ/σ_D on the applied electric field $E \approx V_{dc}/(r_2 - r_1)$ and numerical simulations of the dc response [2], yielding the inelastic relaxation time τ_{in}^{dc} . Figure 5(b) compares the temperature dependences of the inelastic time obtained in the dc domain and from the dynamics of the nonlinear response (f signal). At high temperatures, both times are close to each other. At lower temperatures, there is a considerable difference between these two times. The dc-domain inelastic time $\tau_{in}^{dc}(T)$ follows $1/T^3$ decrease, while the time τ_{in} is mostly proportional to

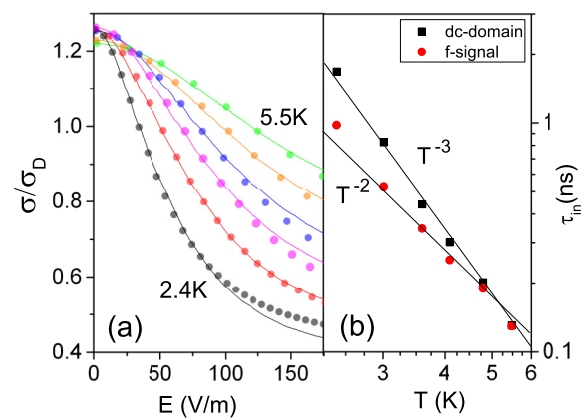


FIG. 5. (Color online) (a) Solid lines present the dependence of the normalized conductivity σ/σ_D on electric field E at different temperatures: 5.5, 4.8, 4.1, 3.6, 3.1, and 2.4 K, from top to bottom. Symbols present simulation of the dc conductivity based on the numerical solution of Eq. (1) using a Gaussian approximation for the electron density of states [2]. (b) Temperature dependences of the inelastic-scattering time obtained in high-frequency experiments (f signal shown in Fig. 4) and from the response in the dc domain shown in (a). $B = 0.333$ T.

$1/T^2$ with a tendency to $1/T^3$ at low temperatures. The observed difference may be related to the effects of an electron redistribution, induced by the dc bias, which are relevant in the dc domain at low temperatures [33,34]. The redistribution mechanism is different from quantal heating and may not be active in the microwave experiments.

The linear temperature dependence of the inelastic-scattering rate $1/\tau_{in}^{SdH}$ observed in SdH experiments at liquid ^4He temperatures [8,14,19] has been attributed to a crossover [14] between Bloch-Grüneisen (BG) and equipartition regimes [18,35]. The dependence is found to be in agreement with the theory [36–39] and direct measurements of the inelastic rate at zero magnetic field [40]. In contrast, thermopower measurements of the electron temperature shows a strong T^3 increase of the inelastic relaxation rate at zero magnetic field, coexisting with the $1/\tau_{in}^{SdH} \sim T$ on the same sample and at the same temperatures [19]. The authors have attributed the discrepancy to a difference in the electron-phonon scattering rate at zero and a strong magnetic fields. Our direct measurements as well as the results obtained in the dc domain [2] indicate the presence of both T^2 and T^3 terms in the inelastic relaxation rate in quantizing magnetic fields. Within an order of magnitude, the cubic term agrees with the one seen in the thermopower experiments [19]. We attribute the T^2 term to $e-e$ scattering [1,2] and the T^3 dependence to the electron-phonon scattering due to the unscreened deformation potential in the BG regime [39,41]. The considerable disagreement with the SdH results indicates, thus, an incompleteness of the accepted interpretation of dc-biased SdH oscillations [8,14,19]. We suggest that the disagreement is related to the resilience of the fundamental harmonic of the SdH amplitude, which is proportional to the Dingle factor, to $e-e$ interaction [42–46]. It causes the relaxation time obtained

from the SdH amplitude to be insensitive to $e-e$ scattering. In contrast, the inelastic time extracted from variations of the total resistance (not SdH amplitude) that are proportional to the square of the Dingle factor is sensitive to $e-e$ scattering [1]. We note that this difference should also lead to a different behavior of electron lifetimes obtained by different methods. In particular, the quantum scattering time obtained from the SdH amplitude [47,48] should not depend on $e-e$ interaction [42–46], whereas the quantum lifetime extracted from the positive quantum magnetoresistance [28] demonstrates a significant contribution from $e-e$ scattering [29].

In conclusion, the dynamics of the nonlinear microwave response of 2D electrons is studied at different temperatures in a GaAs quantum well placed in quantizing magnetic fields. The dynamical response provides the *direct* measurement of the inelastic electron relaxation. When temperature T exceeds the Landau-level separation, the relaxation rate $1/\tau_{in}$ is found to be proportional to T^2 , indicating the electron-electron interaction as the dominant mechanism limiting the nonlinearity. At lower temperatures, the rate tends to be proportional to T^3 , indicating a reduction of the $e-e$ contribution and the important role of the electron-phonon scattering in the inelastic relaxation. The temperature dependence of the relaxation time is found to be significantly different from the one obtained from dc-biased SdH oscillations, indicating an incompleteness of the widely accepted interpretation of this phenomenon.

This work was supported by the National Science Foundation (Division of Material Research - 1104503), the Russian Foundation for Basic Research (Project No. 14-02-01158), and the Ministry of Education and Science of the Russian Federation.

-
- [1] I. A. Dmitriev, M. G. Vavilov, I. L. Aleiner, A. D. Mirlin, and D. G. Polyakov, *Phys. Rev. B* **71**, 115316 (2005).
- [2] J. Q. Zhang, S. Vitkalov, and A. A. Bykov, *Phys. Rev. B* **80**, 045310 (2009).
- [3] N. R. Kalmanovitz, A. A. Bykov, S. Vitkalov, and A. I. Toropov, *Phys. Rev. B* **78**, 085306 (2008).
- [4] A. A. Bykov, Jing-Qiao Zhang, Sergey Vitkalov, A. K. Kalagin, and A. K. Bakarov, *Phys. Rev. Lett.* **99**, 116801 (2007).
- [5] A. A. Bykov, Sean Byrnes, Scott Dietrich, Sergey Vitkalov, I. V. Marchishin, and D. V. Dmitriev, *Phys. Rev. B* **87**, 081409(R) (2013).
- [6] I. A. Dmitriev, A. D. Mirlin, D. G. Polyakov, and M. A. Zudov, *Rev. Mod. Phys.* **84**, 1709 (2012).
- [7] A. B. Fowler, F. F. Fang, W. E. Howard, and P. J. Stiles, *Phys. Rev. Lett.* **16**, 901 (1966).
- [8] M. G. Blyumina, A. G. Denisov, T. A. Polyanskaya, I. G. Savel'ev, A. P. Senichkin, and Yu. V. Shmartsev, *JETP Lett.* **44**, 331 (1986).
- [9] K. Hirakawa and H. Sakaki, *Appl. Phys. Lett.* **49**, 889 (1986).
- [10] S. J. Manion, M. Artaki, M. A. Emanuel, J. J. Coleman, and K. Hess, *Phys. Rev. B* **35**, 9203 (1987).
- [11] A. M. Kreschuk *et al.*, *Solid State Commun.* **65**, 1198 (1988).
- [12] M. J. Barlow, B. K. Ridley, M. J. Kane, and S. J. Bass, *Solid State Electron.* **31**, 501 (1988).
- [13] D. R. Leadley, R. J. Nicholas, J. J. Harris, and C. T. Foxon, *Semicond. Sci. Technol.* **4**, 879 (1989).
- [14] Y. Ma, R. Fletcher, and E. Zaremba, M. D'Iorio, C. T. Foxon, and J. J. Harris, *Phys. Rev. B* **43**, 9033 (1991).
- [15] R. Fletcher, J. J. Harris, C. T. Foxon, and R. Stoner, *Phys. Rev. B* **45**, 6659 (1992).
- [16] D. R. Leadley, R. J. Nicholas, W. Xu, F. M. Peeters, J. T. Devreese, J. Singleton, J. A. A. J. Perenboom, L. van Bockstal and F. Herlach, C. T. Foxon, and J. J. Harris, *Phys. Rev. B* **48**, 5457 (1993).
- [17] N. Balkan, H. Celik, A. J. Vickers, and M. Cankurtaran, *Phys. Rev. B* **52**, 17210 (1995).
- [18] Edmond Chow, H. P. Wei, S. M. Girvin, and M. Shayegan, *Phys. Rev. Lett.* **77**, 1143 (1996).
- [19] N. J. Appleyard, J. T. Nicholls, M. Y. Simmons, W. R. Tribe, and M. Pepper, *Phys. Rev. Lett.* **81**, 3491 (1998).
- [20] Y. S. Gui, C. R. Becker, J. Liu, M. Konig, V. Daumer, M. N. Kiselev, H. Buhmann, and L. W. Molenkamp, *Phys. Rev. B* **70**, 195328 (2004).

- [21] C. Prasad, D. K. Ferry, and H. H. Wieder, *Semicond. Sci. Technol.* **19**, S60 (2004).
- [22] B. I. Halperin, *Phys. Rev. B* **25**, 2185 (1982).
- [23] M. Buttiker, *Phys. Rev. B* **38**, 9375 (1988).
- [24] A. D. Chepelianskii, J. Laidet, I. Farrer, D. A. Ritchie, K. Kono, and H. Bouchiat, *Phys. Rev. B* **90**, 045301 (2014).
- [25] Yonatan Dubi and Massimiliano Di Ventra, *Rev. Mod. Phys.* **83**, 131 (2011).
- [26] S. Jezouin, F. D. Parmentier, A. Anthore, U. Gennser, A. Cavanna, Y. Jin, and F. Pierre, *Science* **342**, 601 (2013).
- [27] Comparison of the sample magnetoresistance $R(B) = R_c + \gamma/\sigma(B)$ at small magnetic fields ($B < 0.1$ T) with Drude formula for the conductivity $\sigma(B)$: $\sigma_D(B) = \sigma_D(0)/[1 + (\omega_c \tau_{ir})^2]$ yields the transport scattering time τ_{ir} and the Drude conductivity $\sigma_D(0)$ at zero magnetic field. Here, $\gamma \approx (r_2 - r_1)/2\pi r_1$ is the geometric factor for the Corbino sample. The comparison indicates that the contact resistance of the sample R_c is below 1 Ohm and is negligible in presented experiments.
- [28] M. G. Vavilov and I. L. Aleiner, *Phys. Rev. B* **69**, 035303 (2004).
- [29] Scott Dietrich, S. A. Vitkalov, D. V. Dmitriev, and A. A. Bykov, *Phys. Rev. B* **85**, 115312 (2012).
- [30] C. L. Yang, J. Zhang, R. R. Du, J. A. Simmons, and J. L. Reno, *Phys. Rev. Lett.* **89**, 076801 (2002).
- [31] A. A. Bykov, J. Q. Zhang, S. A. Vitkalov, A. K. Kalagin, and A. K. Bakarov, *Phys. Rev. B* **72**, 245307 (2005).
- [32] M. G. Vavilov, I. L. Aleiner, and L. I. Glazman, *Phys. Rev. B* **76**, 115331 (2007).
- [33] Scott Dietrich, Sean Byrnes, Sergey Vitkalov, D. V. Dmitriev, and A. A. Bykov, *Phys. Rev. B* **85**, 155307 (2012).
- [34] Scott Dietrich, Sean Byrnes, Sergey Vitkalov, A. V. Goran, and A. A. Bykov, *J. Appl. Phys.* **113**, 053709 (2013).
- [35] H. L. Stormer, L. N. Pfeiffer, K. W. Baldwin, and K. W. West, *Phys. Rev. B* **41**, 1278 (1990).
- [36] P. J. Price, *J. Appl. Phys.* **53**, 6863 (1982).
- [37] P. J. Price, *Solid State Commun.* **51**, 607 (1984).
- [38] V. Karpus, *Sov. Phys. Semicond.* **22**, 268 (1988).
- [39] V. Karpus, *Semicond. Sci. Technol.* **5**, 691 (1990).
- [40] A. A. Verevkin, N. G. Ptitsina, G. M. Chulcova, G. N. Goltsman, E. M. Gershenson, and K. S. Yngvesson, *Phys. Rev. B* **53**, R7592 (1996).
- [41] A. Sergeev, M. Yu. Reizer, and V. Mitin, *Phys. Rev. Lett.* **94**, 136602 (2005).
- [42] G. W. Martin, D. L. Maslov, and M. Y. Reizer, *Phys. Rev. B* **68**, 241309(R) (2003).
- [43] Fowler and R. E. Prange, *Physics (NY)* **1**, 315 (1965)
- [44] S. Engelsberg and G. Simpson, *Phys. Rev. B* **2**, 1657 (1970).
- [45] Y. Adamov, I. V. Gornyi, and A. D. Mirlin, *Phys. Rev. B* **73**, 045426 (2006).
- [46] I. A. Dmitriev, M. Khodas, A. D. Mirlin, D. G. Polyakov, and M. G. Vavilov, *Phys. Rev. B* **80**, 165327 (2009).
- [47] P. T. Coleridge, R. Stoner, and R. Fletcher, *Phys. Rev. B* **39**, 1120 (1989).
- [48] P. T. Coleridge, *Phys. Rev. B* **44**, 3793 (1991).